American Journal of Science and Technology
2014; 1(1): 30-35
Published online March 30, 2014 (http://www.aascit.org/journal/ajst)

Keywords
Mathematical Modeling,
Mathematics of Heart,
Left Ventricular Modeling of Heart,
Direction of Blood Flow Path Inside the Left Ventricle of Heart,
Cardiac Digital Image Processing Mathematically Based Software,
Virtual Heart

Received: February 08, 2014
Revised: March 17, 2014
Accepted: March 18, 2014

A research proposal in mathematical modeling applied to heart and mathematical concepts of mechanisms of heart

Mersedeh Karvandi[1, *], Saeed Ranjbar[1], Mehrdad Shahshahani[2], Arash Rastegar[2], Seyed Ahmad Hassantash[3], Mahnoosh Foroughi[3], Fariba Ranjbar[4]

[1]Taleghani Hospital, ShahidBeheshti University of Medical Sciences, Tehran, Iran
[2]School of Mathematics, Statistics and Computer Sciences of Sharif University of technology, Tehran Iran
[3]Modarres Hospital, Institute of Cardiovascular Research, ShahidBeheshti University of Medical Science, Tehran, Iran
[4]School of Mathematics, Statistics and Computer Sciences of University of Tehran, Tehran, Iran

Email address
mersedeh_karvandi@ipm.ir (M. Karvandi)

Citation
Mersedeh Karvandi, Saeed Ranjbar, MehrdadShahshahani, Arash Rastegar, Seyed Ahmad Hassantash, Mahnoosh Foroughi, Fariba Ranjbar. A Research Proposal in Mathematical Modeling Applied to Heart and Mathematical Concepts of Mechanisms of Heart. *American Journal of Science and Technology*. Vol. 1, No. 1, 2014, pp. 30-35

Abstract
As stated by Jacques Hadmard in 'science and hypothesis', mathematical creation and mathematical intelligence are not without connection with creation in general and with general intelligence. A great proportion of prominent mathematicians have been creators in other fields. One of the greatest, Gauss, carried out important and classical experiments on magnetism; and Newton's fundamental discoveries in optics are well known. And Leibniz influenced by their mathematical abilities on philosophical ones. The research proposals we propose here, are motivated by our background and previous research, and are supposed to indicate my general directions in forthcoming research. Following Poincare, each research subject is formed by an attempt to link two fields in sciences, in order to contribute to at least one of the two. In this proposal, always the mathematical part is the part which takes the benefit. We will try to explain an abstract for each problem and give motivations for importance of the corresponding research direction together with a prediction of expected progress. We hope that the expository style of this proposal does not hurt the scientific value of its predictions. This proposal is addressed to experts in mathematical modeling applied to medicine.

1. A Novel Mathematical Based Software for Modeling the Left Ventricular Myocardium

Purpose: Currently, an echocardiogram presents the left ventricle (LV) of the heart based on images obtained from ultrasound methods. Utilizing mathematical equations, specific echocardiographic data may provide more detailed, valuable and practical information for physicians. In our project using appropriate mathematically

based software, we have attempted to create a novel software capable of demonstrating LV model in normal hearts.

Methods: Echocardiography was performed on 70 healthy volunteers. Data evaluated included: velocity (radial, longitudinal, rotational and vector point), displacement (longitudinal and rotational), strain rate (longitudinal and circumferential) and strain (radial, longitudinal and circumferential) of all 16 LV myocardial segments. Using these data, force vectors of myocardial samples were estimated by MATLAB and LSDYNA softwares. Dynamic orientation contraction (through the cardiac cycle) of every individual myocardial fiber could be created by adding together the sequential steps of the multiple fragmented sectors of that fiber.

This way we attempted to mechanically illustrate the global LV model.

Results: LV Myocardial modeling of the heart: Our study shows that in normal cases myocardial fibers initiate from the posterior-basal region of the heart, continues through the LV free wall, reaches the septum, loops around the apex, ascends, and ends at the superior-anterior edge of LV.

Conclusion: We were able to define the whole LV myocardial model mathematically based on echocardiography, by MATLAB software and LSDYNA software in normal subjects. This will enable physicians to diagnose and follow-up many cardiac diseases when this software is interfaced within echocardiographic machines (Figure 1)[1-12].

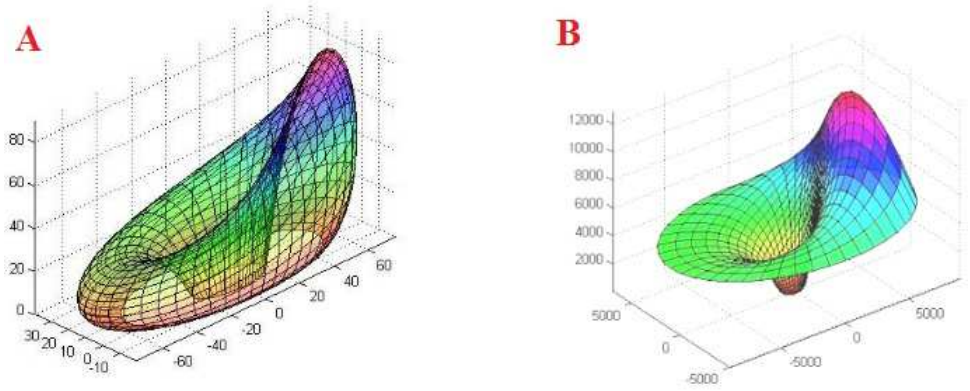

Figure 1. *Myofibers of left ventricular wall thickening and tangential shortening near myocardial septum in MATLAB software (A).Mathematical modeling of the left ventricle related to myocardial fiber paths in MATLAB software (B).*

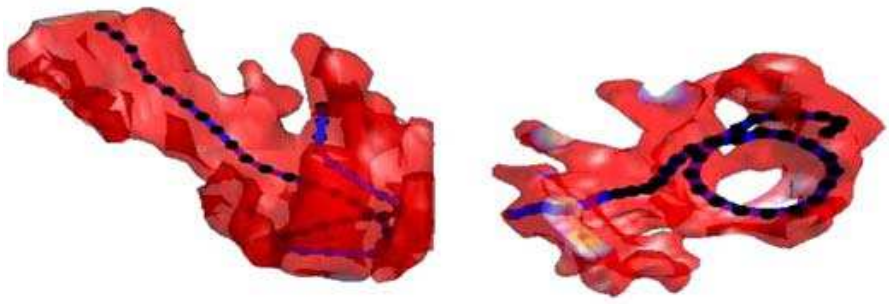

Figure 2. *The rout of a fiber in the left ventricle.*

Mathematical formulations and blood-wall interactions:

We model the blood flow curves inside the left ventricle by studying the flow of the blood curves near echocardiography samples i.e. the basal, mid and apical Anterior and the basal, mid and apical Inferior and the basal , mid and apical Lateral and the basal, mid and apical Septum. these samples as the material elastic points in the myocardium of the left ventricle induce mechanical parameters to the blood of viscosity μ, where we formulate them at this research and calculate them numerically and then apply then in Navier-Stocks equations to model the blood flow curve regionally and globally inside the left ventricle. we have given geometrical modeling of the basal, mid and apical Anterior at the Mathlab software by the following way: be strain components re by the following way: for the mid and apical Anterior d. responded regions where have been named e let $\varepsilon_{rr,P_{bA}}$, $\varepsilon_{ll,P_{bA}}$and $\varepsilon_{cc,P_{bA}}$be strain components of the basal AnteriorP_{bA}, we set

$$\gamma_{P_{bA}} = \{each\ myocardial\ sample\ X\ that\ \varepsilon_{rr,X} \times \varepsilon_{ll,X} = \varepsilon_{rr,P_{bA}} \times \varepsilon_{ll,P_{bA}}\ and$$

$$\varepsilon_{rr,X} \times \varepsilon_{ll,X} \times \varepsilon_{cc,X} = \varepsilon_{rr,P_{bA}} \times \varepsilon_{ll,P_{bA}} \times \varepsilon_{cc,P_{bA}}\}$$

In fact $\gamma_{P_{bA}}$ is that myofiber band in the myocardium where have been shown at Figure 2, And Q's (fiber's algebraic equation) at Figure 2 have the following algebraic equations:

$$Q_{P_{bA}}: D_{P_{bA}} = \left(\sum_{k,l} \varepsilon_{rr}{}'_{P_k,P_l}\, dt\right).{y_1}^2 + \left(\sum_{k,l} \varepsilon_{ll}{}'_{P_k,P_l}\, dt\right).y_2^2 + \left(\sum_{k,l} \varepsilon_{cc}{}'_{P_k,P_l}\, dt\right).y_3^2$$

Where $P_k\ and P_l$ are points belong to $\gamma_{P_{bA}} \cap \mathrm{O}_{P_{bA}}$ and if $P_{bA} = (y_{1,bA}, y_{2,bA}, y_{3,bA})$as the Cartesian coordinate then:

$$D_{P_{bA}} = \left(\sum_{k,l} \varepsilon_{rr}{}'_{P_k,P_l}\, dt\right).{y_{1,bA}}^2 + \left(\sum_{k,l} \varepsilon_{ll}{}'_{P_k,P_l}\, dt\right).y_{2,bA}^2 + \left(\sum_{k,l} \varepsilon_{cc}{}'_{P_k,P_l}\, dt\right).y_{3,bA}^2$$

We consider the surface:

$$F_{P_{bA}}((y_1,y_2,y_3)) = \left(\sum_{k,l} \varepsilon_{rr}{}'_{P_k,P_l}\, dt\right).{y_1}^2 + \left(\sum_{k,l} \varepsilon_{ll}{}'_{P_k,P_l}\, dt\right).y_2^2 + \left(\sum_{k,l} \varepsilon_{cc}{}'_{P_k,P_l}\, dt\right).y_3^2 - D_{P_{bA}}$$

In the region $\mathrm{O}_{P_{bA}}$, let $\varphi_{1,P_{bA}}(t)\,, \varphi_{2,P_{bA}}(t)\ and\ \varphi_{3,P_{bA}}(t)$ are parametrized forms of the projections of the surface $F_{P_{bA}}$ on xy-axis , xz-axis and yz-axis:

$\varphi_{1,P_{bA}}(t) =$
$\left(t, ((D_{P_{bA}} - \left(\sum_{k,l} \varepsilon_{rr}{}'_{P_k,P_l}\, dt\right) t^2)/\left(\sum_{k,l} \varepsilon_{ll}{}'_{P_k,P_l}\, dt\right))^{\frac{1}{2}}\right)$;

$\varphi_{2,P_{bA}}(t) = \left(t, ((D_{P_{bA}} - \left(\sum_{k,l} \varepsilon_{rr}{}'_{P_k,P_l}\, dt\right) t^2)/$
$k,l\varepsilon cc'Pk,Pldt)12;$

$\varphi_{3,P_{bA}}(t) = \left(t, ((D_{P_{bA}} - \left(\sum_{k,l} \varepsilon_{ll}{}'_{P_k,P_l}\, dt\right) t^2)/\left(\sum_{k,l} \varepsilon_{cc}{}'_{P_k,P_l}\, dt\right))^{\frac{1}{2}}\right)$;

Now we set the following formulas:

$T_{1,P_{bA}}(t) = \varphi_{1,P_{bA}}(t)'\ /\left|\varphi_{1,P_{bA}}(t)'\right|$;
$s_{1,P_{bA}} = \int_{t_o}^{t} \varphi_{1,P_{bA}}(u)'\, du$;
$\kappa_{1,P_{bA}}(t).N_{1,P_{bA}}(t) = \frac{dT_{1,P_{bA}}}{ds}$;
$\kappa_{1,P_{bA}}(t) = ((D_{P_{bA}} - \left(\sum_{k,l} \varepsilon_{rr}{}'_{P_k,P_l}\, dt\right) t^2)/\left(\sum_{k,l} \varepsilon_{ll}{}'_{P_k,P_l}\, dt\right))^{\frac{1}{2}})'' - 0/{s_{1,P_{bA}}}'^3$;
$a_{1,P_{bA}}(t) = {s_{1,P_{bA}}}''.\ T_{1,P_{bA}}(t) + \kappa_{1,P_{bA}}(t).N_{1,P_{bA}}(t)$;
$T_{2,P_{bA}}(t) = \varphi_{2,P_{bA}}(t)'\ /\left|\varphi_{2,P_{bA}}(t)'\right|$;
$s_{2,P_{bA}} = \int_{t_o}^{t} \varphi_{2,P_{bA}}(u)'\, du$;
$\kappa_{2,P_{bA}}(t).N_{2,P_{bA}}(t) = \frac{dT_{2,P_{bA}}}{ds}$;
$\kappa_{2,P_{bA}}(t) = ((D_{P_{bA}} - \left(\sum_{k,l} \varepsilon_{rr}{}'_{P_k,P_l}\, dt\right) t^2)/\left(\sum_{k,l} \varepsilon_{cc}{}'_{P_k,P_l}\, dt\right))^{\frac{1}{2}})'' - 0/{s_{2,P_{bA}}}'^3$;
$a_{2,P_{bA}}(t) = {s_{2,P_{bA}}}''.\ T_{2,P_{bA}}(t) + \kappa_{2,P_{bA}}(t).N_{2,P_{bA}}(t)$;
$T_{3,P_{bA}}(t) = \varphi_{3,P_{bA}}(t)'\ /\left|\varphi_{3,P_{bA}}(t)'\right|$;
$s_{3,P_{bA}} = \int_{t_o}^{t} \varphi_{3,P_{bA}}(u)'\, du$;
$\kappa_{3,P_{bA}}(t).N_{3,P_{bA}}(t) = \frac{dT_{3,P_{bA}}}{ds}$;
$\kappa_{3,P_{bA}}(t) = ((D_{P_{bA}} - \left(\sum_{k,l} \varepsilon_{ll}{}'_{P_k,P_l}\, dt\right) t^2)/\left(\sum_{k,l} \varepsilon_{ll}{}'_{P_k,P_l}\, dt\right))^{\frac{1}{2}})'' - 0/{s_{3,P_{bA}}}'^3$;
$a_{3,P_{bA}}(t) = {s_{3,P_{bA}}}''.\ T_{3,P_{bA}}(t) + \kappa_{3,P_{bA}}(t).N_{3,P_{bA}}(t)$;

If (x_1, x_2, x_3, t) be the coordinate system of the red blood cell in a neighborhood $\mathrm{O}_{P_{bA}}$ of the basal Anterior and $\delta(x_1, x_2\ ,\ x_3, t) = \delta^*(x_1,t).\delta^*(x_2,t).\delta^*(x_3,t)$ where $\delta^* is the diracfunction$. And $C_{1,P_{bA}}, C_{2,P_{bA}}\ and\ C_{3,P_{bA}}$ be the graphs of $\varphi_{1,P_{bA}}(t), \varphi_{2,P_{bA}}(t)\ and\ \varphi_{3,P_{bA}}(t)$ respectively, then the mechanical parameters of the red blood cells (RBC) in the region $\mathrm{O}_{P_{bA}}$ are realized by the following formulas:

$v_{1,P_{bA}}(t) = \int_{C_{1,P_{bA}}} T_{1,P_{bA}}(t) \otimes \delta(x_1,x_2,x_3,t)dt$;
$n_{1,P_{bA}}(t) = \int_{C_{1,P_{bA}}} N_{1,P_{bA}}(t) \otimes \delta(x_1,x_2,x_3,t)dt$;
$a^{RBC}_{1.P_{bA}}(\mathrm{t}) = \int_{C_{1,P_{bA}}} a_{1,P_{bA}}(t) \otimes \delta(x_1,x_2,x_3,t)dt$;
$v_{2,P_{bA}}(t) = \int_{C_{2,P_{bA}}} T_{2,P_{bA}}(t) \otimes \delta(x_1,x_2,x_3,t)dt$;
$n_{2,P_{bA}}(t) = \int_{C_{2,P_{bA}}} N_{2,P_{bA}}(t) \otimes \delta(x_1,x_2,x_3,t)dt$;
$a^{RBC}_{2.P_{bA}}(\mathrm{t}) = \int_{C_{2,P_{bA}}} a_{1,P_{bA}}(t) \otimes \delta(x_1,x_2,x_3,t)dt$;
$v_{3,P_{bA}}(t) = \int_{C_{3,P_{bA}}} T_{3,P_{bA}}(t) \otimes \delta(x_1,x_2,x_3,t)dt$;
$n_{3,P_{bA}}(t) = \int_{C_{1,P_{bA}}} N_{3,P_{bA}}(t) \otimes \delta(x_1,x_2,x_3,t)dt$;
$a^{RBC}_{3.P_{bA}}(\mathrm{t}) = \int_{C_{3,P_{bA}}} a_{1,P_{bA}}(t) \otimes \delta(x_1,x_2,x_3,t)dt$;

In fact these formulas give an analytical solution of the Navier-Stocks equations in the region $\mathrm{O}_{P_{bA}}$ of the basal Anterior. Almost, the same argument is for the other echocardiographic segments [12].

2. A Novel Mathematical Based Software to Demonstrate Flow Direction and Curves Inside the Left Ventricular Myocardium

Purpose: Demonstration of blood flow direction inside cardiac chambers can provide valuable information in

normal subjects and pathologic cardiac processes. In our center we have already created a software able to generate the left ventricle (LV) model, the most important chamber of the heart. In this project we have attempted to define blood flow pattern in LV.

Methods: The study was conducted on 70 healthy volunteers in whom their LV models were already determined, based on their echocardiograpic data. This information along with blood flow parameters including: local interacted force with the myocardial segments, velocity vectors (local radial, local longitudinal and local circumferential), local relative strength of blood with the 16 myocardial segments (radial, longitudinal and circumferential) and curvature index were defined and used as input into algorithm to solve the partial deferential Navier-Stocks equations. For all calculations average mean ± standard deviation was used.

Results: In the LV blood flows through the mitral valve, hits the lateral LV free wall, turbulences clockwise at the apex of the heart, hits the septal wall and flows towards the aortic valve.

Conclusion: For the first time we have innovated a novel software that shows complete blood flow path inside the LV. Detailed information can be obtained about heart function by interfacing the related software within the echocardiograph machine. This innovation also opens doors to much more research in the heart chambers in normal and diseased hearts (Figure 3). [13-17].

3. Impact of Prosthetic Mitral Valve Direction on Blood Flow Path Inside the left Ventricle

Purpose: The ideal prosthetic mitral valve (PMV) replacement should restore near normal hemodynamics, and offer the best chance for regression or remodeling from the effects of the primary mitral valve disease. We present our result of the evaluation of blood flow curves inside the left ventricle (LV).

Method: The direction of blood flow inside the LV starting with the mitral valve and ending up to the aortic valve was determined by sophisticated mathematical/physical models: modeling of LV, then using fluid mechanical (Navier-Stocks) equations through spectral theory. The study included 3 groups of patients. First: 70 healthy volunteers. Second: 10 patients with PMV replacement with the direction of the leaflets positioned as the direction of native mitral leaflets (anatomic PMV). Third: 10 patients with their PMV perpendicular to the direction of native mitral valves (anti-anatomic PMV).

Result: As demonstrated in the diagram flow direction inside the LV is completely different from each other when the two perpendicular valve directions are chosen as much as when compared with the normal heart. In a normal LV Initial pressure force is impacted on the free wall in the contrary to when an anatomically directed PMV is performed with initial pressure impacted to LV inter-septum. When the PMV is directed in an anti-anatomic position the initial pressure is divided to both septum and LV free wall.

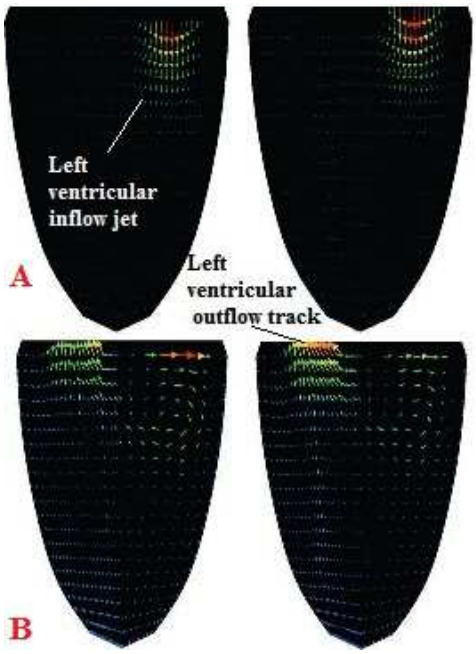

Figure 3. *In the late filling phase that was characterized by an irrotational flow obscuring the vortex. This was followed by in the early isovolumic contraction (IVC) period (A), the vortex was relocated in the proximity of the anterior mitral leaflet in the LVOT region (B). During the late IVC period, the vortex persisted in the left ventricular outflow tract region and directed flow towards aortic valve.*

Conclusion: This study demonstrates that different flow directions are resulted when different directions of the prosthetic valve are chosen. The impact of these distinct directions of blood flow along with different pressure forces applied to different areas of the LV may be a strong contributing factor to unwanted remodeling of the heart, which requires further long term studies (Figure 4) [18-20].

4. Achievability of the Assessment of the Mitral Valve Leaflets by Mathematical Equations of Inelasticity based on Echocardiography

Purpose: The mechanics of the mitral valve (MV) leaflet as a nonlinear, inelastic and anisotropic soft tissue results from an integrated response of many mathematical/physical indicators that illustrate the tissue. It is essential to calculate velocity, displacement, strain rate and strain at a component level that is to work at the cellular level. In this study we developed the first three dimensional displacement vectors field in the characterization of mitral valve leaflets (MVLs) in continuum equations of inelasticity framework based on echocardiography.

Method: Echocardiography imaging of the MV motion during the cardiac cycle in transthoracic echocardiogram (TTE) planes and multiplane transesophageal echocardiography (TEE) in the lower esophageal views at 0,10,15,30, 45-60, 75, 80, 90, 110-125 and 135 degrees, were prospectively acquired in 200 patients at 65 time-frames from diastole to systole (early diastole, mid diastole, atrial systole, late diastole, end systole). In each plane and for each frame during cardiac cycle, MV annulus and leaflets, and bases, middles and tips of anterior mitral valve leaflet (AML) and posterior mitral valve leaflet (PML), were manually identified using MATLAB software. Then, 3-D MV annulus geometry, leaflets' measurements, AML and PML positions were automatically computed for each frame, and used as input to displacement vectors modeling of MVLs. By solving mathematical equations of inelastic properties of leaflets, each plane was replaced with 60 vectors of displacement and ultimately MVLs were realized by 1125 vectors of displacements where demonstrate translations, rotations and pure strains of bases, middles and tips of AML and PML per cardiac cycle.

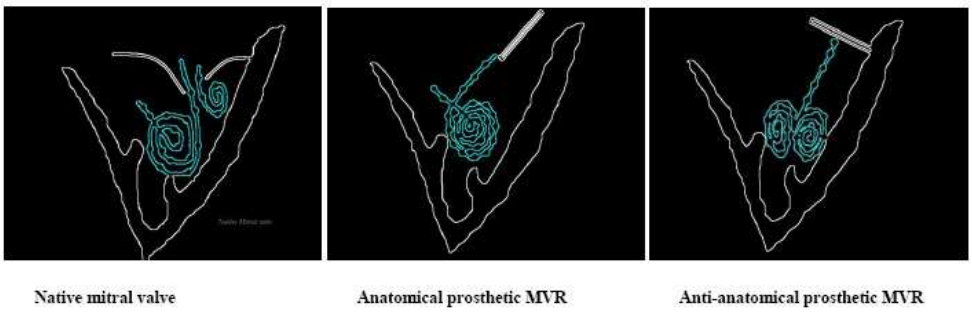

Figure 4. *Impact of prosthetic mitral valve direction on blood flow path inside the left ventricle.*

Result: Preliminary results concerning a different aspect of MVLs biomechanics, such as leaflets dynamics, displacements, velocities, strain rates and strains of points on leaflets, were in good agreement within echocardiographic observations (Figure 5).

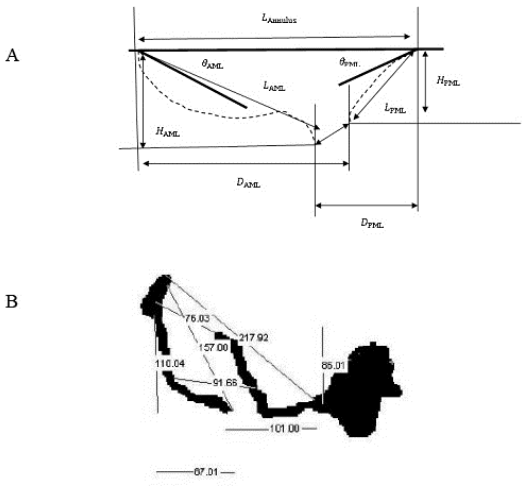

Figure 5. *Parameters used to define the geometry of Mitral valve. B) The numerical calculation of geometric parameters of a mitral valve in MATLAB software.*

Conclusion: Quantitative information on MVLs and dynamics can be extracted from equations of inelasticity, when performed in multiple TTE and TEE planes. These data potentially allow the implementation of an image-based approach for patient-specific modeling of MVLs. This approach could overcome the limitations of previously proposed models and give new insight into the complex MV function. This approach could constitute the basis for accurate evaluation of MV pathologic conditions and for the planning of surgical procedures [21].

Disclosure

There is no conflict of interest.

References

[1] Kim HK, Sohn DW, Lee SE, Choi SY, Park JS, Kim YJ. Assessment of left ventricular rotation and torsion with two-dimensional speckle tracking echocardiography. J Am SocEchocardiogr 2007; 20:45–53.

[2] Zhou Z, Ashraf M, Hu D, Dai X, Xu Y, Kenny B. Three-dimensional speckle tracking imaging for left ventricular rotation measurement. An in vitro validation study. J Ultrasound Med 2010; 29:3–9.

[3] Le Grice IJ, Takayama Y, Covell JW. Transverse shear along myocardial cleavage planes provides a mechanism for normal systolic wall thickening. Circ Res 1995; 77: 182–193.

[4] Seo Y, Ishizu T, Enomoto Y, Sugimori H, Yamamoto M, Machino T. Validation of 3-dimensional speckle tracking imaging to quantify regional myocardial deformation. CircCardiovasc Imaging 2009; 2:1–9.

[5] Moore CC, Lugo-Olivieri CH, McVeigh ER, Zerhouni EA. Three dimensional systolic strain patterns in the normal human left ventricle: characterization with tagged MR imaging. Radiology 2000; 214: 453–466.

[6] Truesdell C.A. A critical summary of developments in nonlinear elasticity. Journal of rational mechanics, 1952; 1:125-300.

[7] Truesdell C.A. A critical summary of developments in nonlinear elasticity. Journal of rational mechanics, 1953; 2: 593-616.

[8] Heimdal A. 4D Strain: Advanced research application for quantitative echocardiography. GE Healthcare. 2011.

[9] D'hooge, J., Heimdal, A., Jamal, F., Kukulski, T., Bijnens, B., Rademakers, F., Hatle, L., Suetens, P., Sutherland, G.R. "Regional strain and strain rate measurements by cardiac ultrasound: principles, implementation and limitations." Eur J Echocardiogr 2000; 1:70-154.

[10] Badano LP, Lang RM, Zamorano JL Textbook of Real-Time Three-Dimensional Echocardiography. Springer-Verlag London Ltd, London, 2011

[11] Le Grice I, Hunter P, Young A, Small B. The architecture of the heart: a data-based model. Philos Trans R SocLond A Math PhysSci 2001; 35: 1217–1232.

[12] Ranjbar S. Karvandi M. Ajzachi M. System and method modeling left ventricle of heart. US Patent 2013; patent number 8,414,490.

[13] Geu-Ru Hong G. R., Pedrizzetti G., Giovanni Tonti G et al. Characterization and quantification of Vortex Flow in the Human Left Ventricle by contrast echocardiography using vector particle Image velocimetry.JACC: Cardiovascular imaging. 2008; 1: 705-717.

[14] A, Houle H., Pedrizzetti G., Tonti G et al. Echocardiographic Particle Image Velocimetry: A novel technique for quantification of left ventricular blood vorticity pattern. J Am SocEchocardiogr. 2010; 23: 86- 94.

[15] Belohlavek M. Vortex formation time: an emerging echocardiographic index of left ventricular filling efficiency? European Heart Journal – Cardiovascular Imaging.2012 13: 367–369.

[16] Hendabadi S. Bermejo J. Benito Y et al. Topology of Blood Transport in the Human Left Ventricle by Novel Processing of Doppler Echocardiography. Journal of Annals of Biomedical Engineering.2013; 10: 39-53.

[17] Ranjbar S., Karvandi M., Hassantash S. A. A Novel Mathematical Fluid Dynamic of Left Ventricular Dilated Cardiomyopathy.Poster presentation at AmericanEcho. 2012; Abstract: P2-89.

[18] Re´kaFaludi R. K., SzulikM,hooge Jan D et al. Left ventricular flow patterns in healthy subjects and patients with prosthetic mitral valves: An in vivo study using echocardiographic particle image velocimetry. The Journal of Thoracic and Cardiovascular Surgery.2009 139: 1501-1510.

[19] Van Rijk-Zwikker GL., DelemarreBJ., Huysmans HA. The orientation of the bileafletCarboMedics valve in the mitral position determines left ventricular spatial flow patterns. Eur J Cardiothorac Surg. 1996;10: 13-20.

[20] Kheradvar A., Gharib M. Influence of ventricular pressure drop on mitral annulus dynamics through the process of vortex ring formation. Ann Biomed Eng. 2007; 35: 50-64.

[21] Karvandi M., Ranjbar S., Hassantash S. A. Achievability of the Assessment of the Mitral Valve Leaflets by Mathematical Equations of Inelasticity Based EchocardiographyPoster presentation at Americanecho. 2012; Abstract: P2-92.